

Predictions of water/oil interfacial tension at elevated temperatures and pressures: A molecular dynamics simulation study with biomolecular force fields

Supporting Information

Konstantinos D. Papavasileiou,¹ Othonas A. Mourtos,² and Ioannis G. Economou^{1,3,*}

¹National Center for Scientific Research “Demokritos”, Institute of Nanoscience and Nanotechnology, Molecular Thermodynamics and Modelling of Materials Laboratory, GR-15310 Aghia Paraskevi Attikis, Greece

²Engineering Thermodynamics, Process & Energy Department, Faculty of Mechanical, Maritime and Materials Engineering, Delft University of Technology, Leeghwaterstraat 39, 2628CB Delft, The Netherlands

³Texas A&M University at Qatar, Chemical Engineering Program, Education City, PO Box 23874, Doha, Qatar

*To whom correspondence should be addressed

IGE: ioannis.economou@qatar.tamu.edu

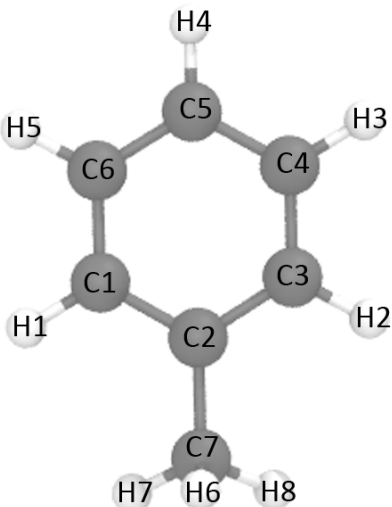
As described in the manuscript, the LJ-PME method was applied for the treatment of long-range Lennard-Jones interactions, as this has been shown to improve the description in inhomogeneous systems such as water/hydrocarbon mixtures [1]. However, it has been found recently that the combination of GAFF and LJ-PME leads to overestimations in the surface tension of organic liquids [2]. The source of this overestimation has been attributed to be the fact that the AMBER force fields, such as GAFF and Lipid14, have been parametrized for long-range Lennard-Jones (LJ) corrections using a simple cut-off approach [2]. Moreover, it has been reported that using the LJ-PME scheme led to an increase of the surface tension in lipid monolayers of almost 25% [3], which is close to the overestimation of IFT in our simulations. Therefore, utilizing the LJ-PME approach, even though it is computationally robust, has not been extensively tested in conjunction with force fields optimized for the cut-off approach [2]. This, however, contradicts the original argument of the LJ-PME developers, who claim that using this method is equivalent to imposing a 16 Å cut-off for the LJ potential [3]. In order to examine whether the IFT values are overestimated as a result of using the LJ-PME treatment, we have performed additional simulations on all systems by employing a 16 Å cut-off.

From the IFT data collected in Table S7, it is deduced that the IFT values are independent of the long-range treatment used for the LJ potential. We therefore chose the LJ-PME method for the simulations presented in the manuscript.

Table S1. Lipid14 and GAFF atom types.

GAFF	Lipid14	Description
c3	cD	sp ³ carbon
ca	—	aromatic carbon
hc	hL	hydrogen bonded to aliphatic carbon without electron withdrawing group
ha	—	hydrogen bonded to aromatic carbon

Table S2. Toluene GAFF atom types and partial charges.



Atom	Type	Charge
C1	ca	-0.275155
C2	ca	0.282982
C3	ca	-0.275155
C4	ca	-0.112135
C5	ca	-0.172188
C6	ca	-0.112135
H1	ha	0.157026
H2	ha	0.157026
H3	ha	0.137677
H4	ha	0.139105
H5	ha	0.137677
C7	c3	-0.384795
H6	hc	0.106690
H7	hc	0.106690
H8	hc	0.106690

Table S3. *n*-dodecane Lipid14 atom types and partial charges.

Atom	Type	Charge
C1	cD	-0.218051
H1	hL	0.043707
H2	hL	0.043707
H3	hL	0.043707
C2	cD	0.184369
H4	hL	-0.030719
H5	hL	-0.030719
C3	cD	-0.081636
H6	hL	0.017473
H7	hL	0.017473
C4	cD	-0.000351
H8	hL	0.010549
H9	hL	0.010549
C5	cD	-0.045994
H10	hL	0.014082
H11	hL	0.014082
C6	cD	-0.016676
H12	hL	0.012224
H13	hL	0.012224
C7	cD	-0.016676
H14	hL	0.012224
H15	hL	0.012224
C8	cD	-0.045994
H16	hL	0.014082
H17	hL	0.014082
C9	cD	-0.000351
H18	hL	0.010549
H19	hL	0.010549
C10	cD	-0.081636
H20	hL	0.017473
H21	hL	0.017473
C11	cD	0.184369
H22	hL	-0.030719
H23	hL	-0.030719
C12	cD	-0.218051
H24	hL	0.043707
H25	hL	0.043707
H26	hL	0.043707

Table S4. TIP4P/2005, TIP3P and SPC/E water atom types and partial charges.

Atom	Type	Charge
TIP4P/2005		
O	OWT4	0.0000
H1	HW	0.5564
H2	HW	0.5564
IW	IW	-1.1128
TIP3P		
O	OW	-0.8340
H1	HW	0.4170
H2	HW	0.4170
SPC/E		
O	OW	-0.8476
H1	HW	0.4238
H2	HW	0.4238

Table S5. GAFF, Lipid14, TIP4P/2005, TIP3P, SPC/E force field parameters employed in the IFT simulations.

Type of interaction	Potential function and parameters		
Bond stretching	$V_b(r_{ij}) = \frac{1}{2} k_{ij}^b (r_{ij} - b_{ij})^2$		
	Bond	k_{ij}^b (kJ mol ⁻¹ nm ⁻²)	b_{ij} (nm)
	c3-c3	2.5363e+05	0.15350
	c3-hc	2.8225e+05	0.10920
	cD-cD	2.5363e+05	0.15350
	cD-hL	2.8225e+05	0.10920
	ca-ca	4.0033e+05	0.13870
	ca-c3	2.7070e+05	0.15130
	ca-ha	2.8811e+05	0.10870
TIP4P/2005	HW-OWT4	4.6275e+05	0.09572
	IW-OWT4	—	0.01546
TIP3P	HW-OW	4.6275e+05	0.09572
SPC/E	HW-OW	3.4500e+05	0.10000
Bond angle bending	$V_a(\theta_{ijk}) = \frac{1}{2} k_{ijk}^\theta (\theta_{ijk} - \theta_{ijk}^0)^2$		
	Bond angle	k_{ijk}^θ (kJ mol ⁻¹ rad ⁻²)	θ_{ijk}^0 (°)
	cD-cD-hL	3.8802e+02	110.05
	cD-cD-cD	5.2894e+02	110.63
	hL-cD-hL	3.2995e+02	108.35
	ca-ca-ca	5.6216e+02	119.97
	c3-ca-ca	5.3421e+02	120.63
	ca-ca-ha	4.0551e+02	120.01
	ca-c3-hc	3.2995e+02	108.35
TIP4P/2005	HW-OWT4-HW	8.3680e+02	104.52
	HW-OWT4-IW	—	52.26
TIP3P	HW-OW-HW	8.3680e+02	104.52
SPC/E	HW-OW-HW	3.8300e+02	109.47
Dihedral angles	$V_d(\varphi_{ijkl}) = k_\varphi (1 + \cos(n\varphi - \varphi_s))$		
	Angle	k_φ (kJ mol ⁻¹)	φ_s (°)
	cD-cD-cD-cD	1.30206	180.0
	cD-cD-cD-cD	-0.51589	180.0
	cD-cD-cD-cD	0.48074	0.0
	cD-cD-cD-cD	-0.92006	0.0
	cD-cD-cD-cD	0.90793	0.0

Table S5. Cont.

Dihedral angles	hL-cD-cD-hL	0.62760	0.0	3				
	cD-cD-cD-hL	0.66944	0.0	3				
$V_d(\varphi_{ijkl}) = \sum_{n=0}^5 C_n (\cos(\psi))^n, \psi = \varphi - 180^\circ, C_n (\text{kJ mol}^{-1})$								
	Angle	C_0	C_1	C_2	C_3	C_4	C_5	
	ca-ca-ca-ca	30.334	0.000	-30.334	0.000	0.000	0.000	
	ca-ca-ca-ha	30.334	0.000	-30.334	0.000	0.000	0.000	
	hc-c3-ca-ca	0.000	0.000	0.000	0.000	0.000	0.000	
	c3-ca-ca-ca	30.334	0.000	-30.334	0.000	0.000	0.000	
	c3-ca-ca-ha	30.334	0.000	-30.334	0.000	0.000	0.000	
	ha-ca-ca-ha	30.334	0.000	-30.334	0.000	0.000	0.000	
Improper dihedral angles	$V_d(\varphi_{ijkl}) = k_\varphi (1 + \cos(n\varphi - \varphi_s))$							
	Angle	k_φ (kJ mol ⁻¹)	φ_s (°)		n			
	ca-ca-ca-ha	4.60240	180.0		2			
	c3-ca-ca-ca	4.60240	180.0		2			
Non bonded Lennard-Jones	$V_{LJ} = 4\epsilon_{ij} \left[\left(\frac{\sigma_{ij}}{r_{ij}} \right)^{12} - \left(\frac{\sigma_{ij}}{r_{ij}} \right)^6 \right]$							
	ca	σ (nm)		ϵ (kJ mol ⁻¹)				
	ha	0.339970		0.35982				
	c3	0.259960		0.06276				
	hc	0.339970		0.45773				
	cD	0.264950		0.06569				
	hL	0.339970		0.45773				
		0.260140		0.04184				
TIP4P/2005	OWT4	0.315890		0.77491				
	HW	0.000000		0.00000				
	IW	0.000000		0.00000				
TIP3P	OW	0.315066		0.63627				
	HW	0.000000		0.00000				
SPC/E	OW	0.316600		0.65000				
	HW	0.000000		0.00000				
Non bonded electrostatic	$V_c(r_{ij}) = \frac{1}{4\pi\epsilon_o\epsilon_r r_{ij}} \frac{q_i q_j}{r_{ij}}$							
	Partial charge values are provided in Tables S2-S4.							

Table S6. Calculated IFT values of our contest entry and benchmark experimental values. The water model used is TIP4P/2005.

T (K)	γ (mN/m)			Difference (%)
water/toluene				
383.15	simulation	32.3 ± 0.4	Experiment	28.6
403.15		29.1 ± 0.6		26.4
423.15		27.5 ± 0.6		23.8
443.15		26.1 ± 0.6		20.2
water/ <i>n</i> -dodecane				
383.15	simulation	47.4 ± 0.8	Experiment	40.0
403.15		44.7 ± 0.5		36.5
423.15		41.7 ± 0.5		32.9
443.15		38.4 ± 0.9		28.5
water/toluene/ <i>n</i> -dodecane				
383.15	simulation	38.5 ± 1.0	Experiment	31.4
403.15		36.4 ± 0.9		29.0
423.15		33.9 ± 0.7		26.1
443.15		31.9 ± 0.8		22.6

Table S7. Calculated IFT values with the LJ-PME approach and 16 Å cut-off treatment of the tail of Lennard-Jones potential. The water model used is TIP4P/2005.

T (K)	γ (mN/m)							
	water/toluene							
383.15	LJ-PME 5 ns (contest entry)	32.3 ± 0.4	LJ-PME 10 ns	33.1 ± 0.7	16 Å cut-off 10 ns	32.0 ± 0.6	Experiment	28.6
403.15		29.1 ± 0.6		31.2 ± 1.0		30.3 ± 0.6		26.4
423.15		27.5 ± 0.6		29.0 ± 0.6		28.6 ± 1.0		23.8
443.15		26.1 ± 0.6		25.6 ± 0.7		25.5 ± 0.4		20.2
	water/n-dodecane							
383.15	LJ-PME 5 ns (contest entry)	47.4 ± 0.8	LJ-PME 10 ns	47.5 ± 0.8	16 Å cut-off 10 ns	47.8 ± 1.3	Experiment	40.0
403.15		44.7 ± 0.5		45.4 ± 0.8		45.3 ± 2.1		36.5
423.15		41.7 ± 0.5		42.4 ± 0.8		42.1 ± 1.4		32.9
443.15		38.4 ± 0.9		39.8 ± 1.1		38.4 ± 0.8		28.5
	water/toluene/n-dodecane							
383.15	LJ-PME 5 ns (contest entry)	38.5 ± 1.0	LJ-PME 10 ns	38.7 ± 0.8	16 Å cut-off 10 ns	38.0 ± 0.7	Experiment	31.4
403.15		36.4 ± 0.9		36.4 ± 0.3		36.0 ± 0.6		29.0
423.15		33.9 ± 0.7		34.7 ± 0.4		33.9 ± 0.4		26.1
443.15		31.9 ± 0.8		31.6 ± 0.9		30.9 ± 0.6		22.6

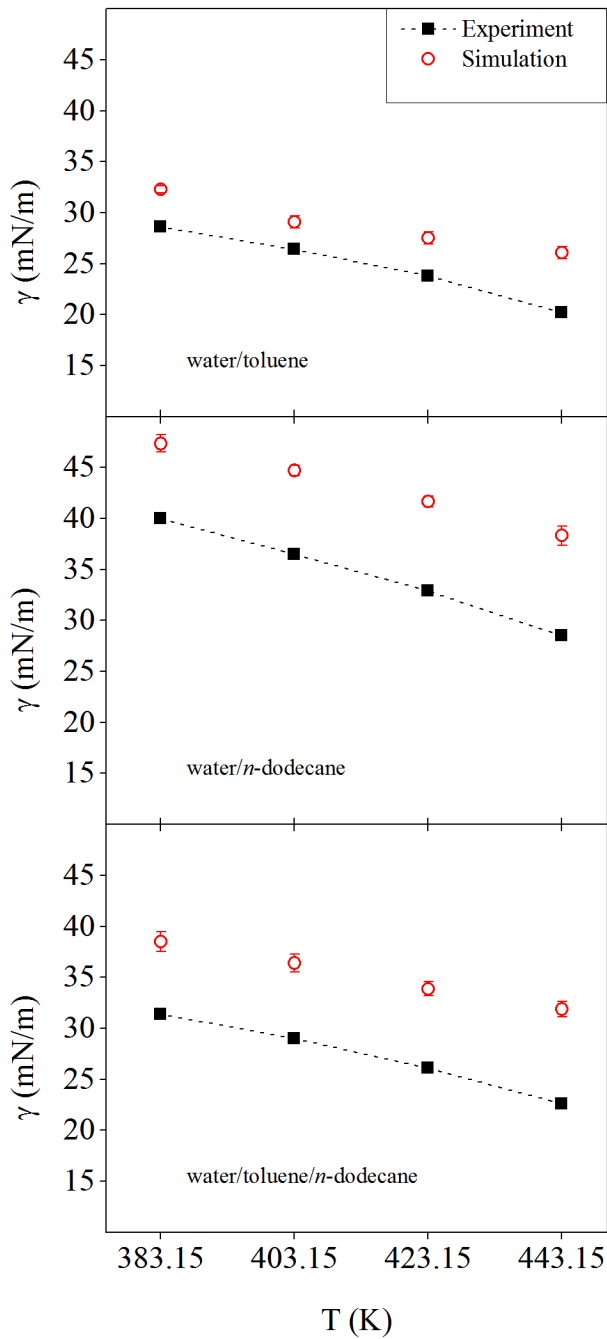


Figure S1. Experimental and calculated interfacial tension values (contest entry) of water/toluene, water/n-dodecane and 50:50 (wt/wt) water/toluene/n-dodecane mixtures with the GAFF (toluene), Lipid14 (*n*-dodecane) and TIP5P/2005 (water) force fields.

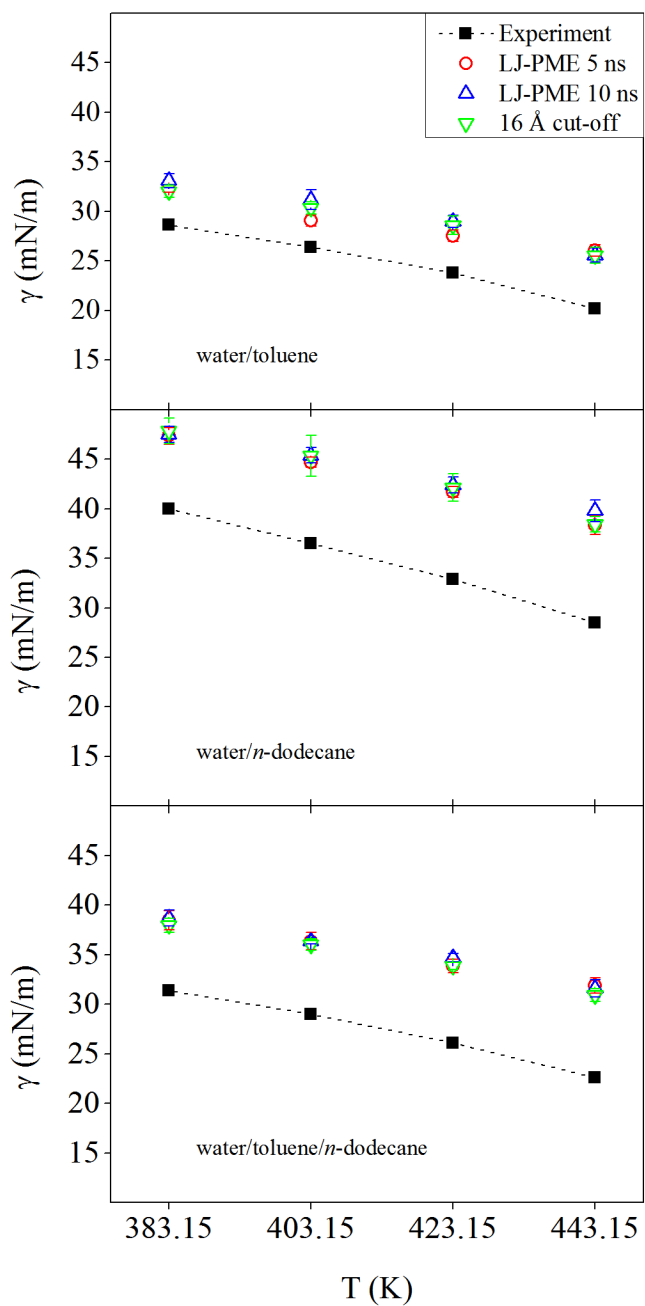


Figure S2. Calculated interfacial tension of water/toluene, water/n-dodecane and 50:50 (wt/wt) water/toluene/n-dodecane mixtures obtained from longer runs (maybe add how many ns) and different treatments of the Lennard-Jones potential.

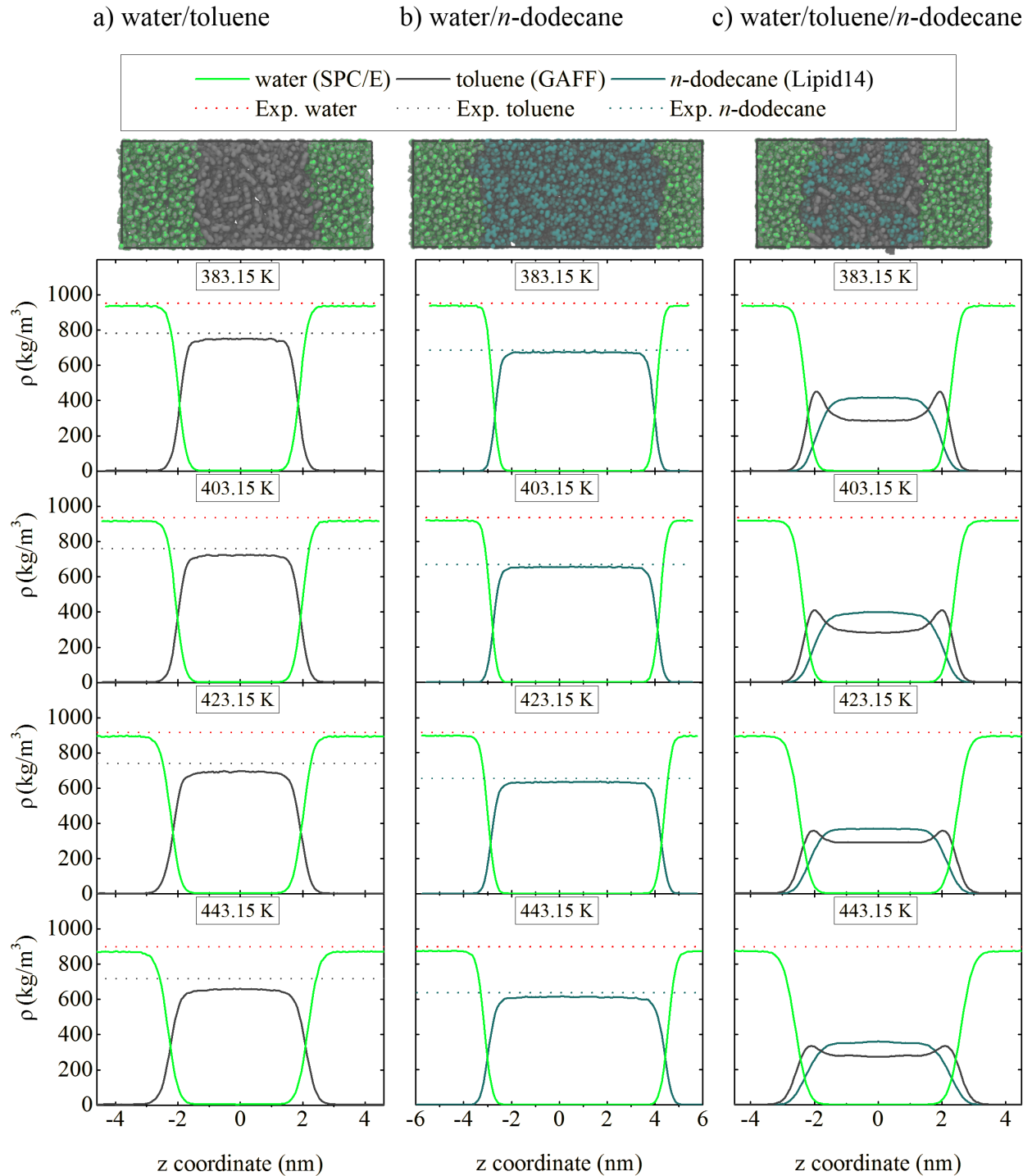


Figure S3. Equilibrated structures and partial densities of all systems studied using the SPC/E model for water, at different temperatures and pressure 1.83 MPa. Water, toluene and *n*-dodecane molecules are illustrated in green, gray and cyan colors, respectively.

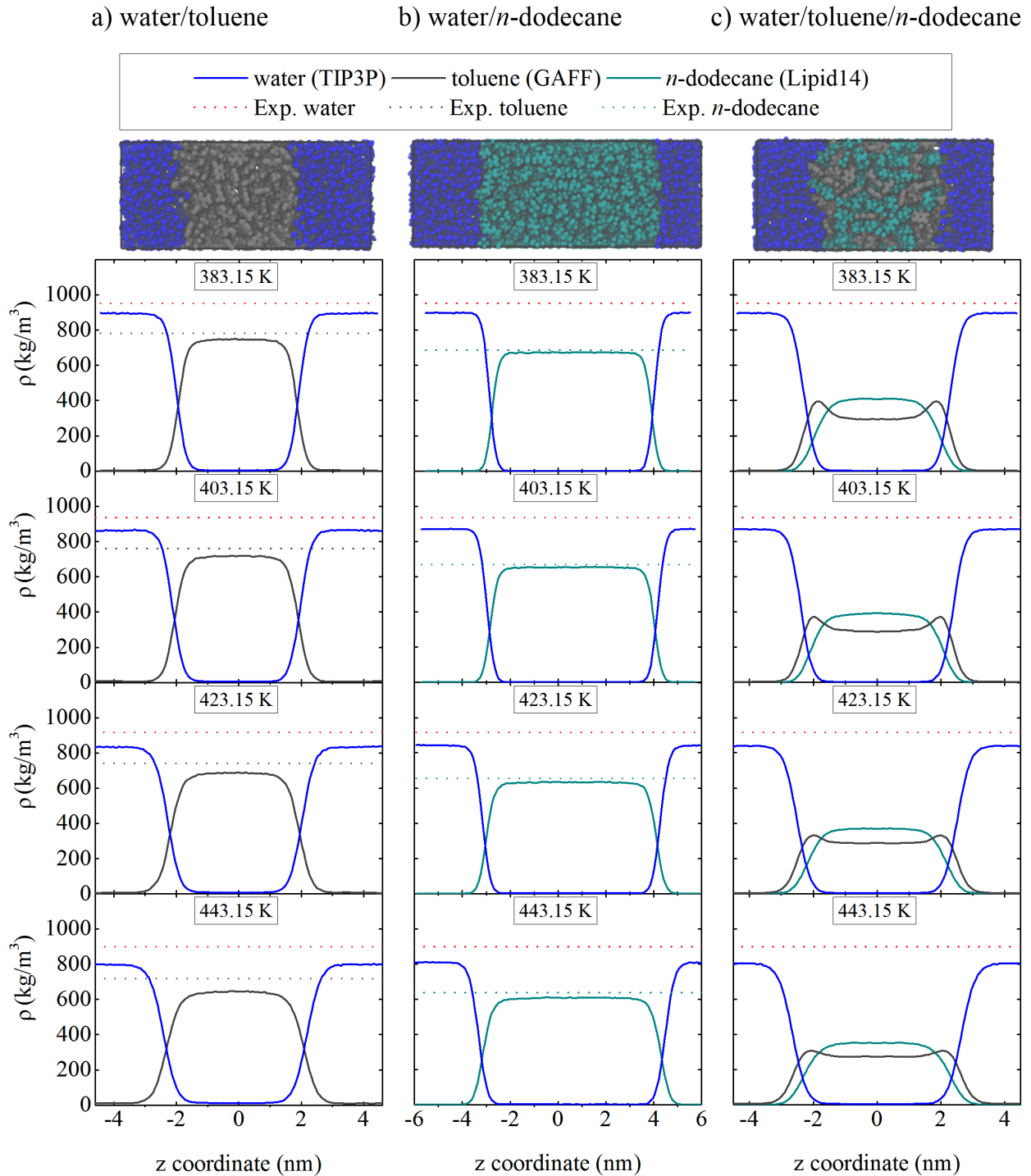


Figure S4. Equilibrated structures and partial densities of all systems studied using the TIP3P model for water, at different temperatures and pressure 1.83 MPa. Water, toluene and *n*-dodecane molecules are illustrated in blue, gray and cyan colors, respectively.

References

- [1] L. Lundberg, O. Edholm, Dispersion corrections to the surface tension at planar surfaces, *J. Chem. Theory Comput.*, 12 (2016) 4025-4032.
- [2] N.M. Fischer, P.J. van Maaren, J.C. Ditz, A. Yildirim, D. van der Spoel, Properties of organic liquids when simulated with long-range Lennard-Jones interactions, *J. Chem. Theory Comput.*, 11 (2015) 2938-2944.
- [3] C.L. Wennberg, T. Murtola, B. Hess, E. Lindahl, Lennard-Jones lattice summation in bilayer simulations has critical effects on surface tension and lipid properties, *J. Chem. Theory Comput.*, 9 (2013) 3527-3537.